

The dyke swarm of Mount Calanna (Etna, Italy): an example of the uppermost portion of a volcanic plumbing system

Carmelo Ferlito · Eugenio Nicotra

Received: 6 March 2008 / Accepted: 11 July 2010 / Published online: 9 September 2010
© Springer-Verlag 2010

Abstract A new multidisciplinary study, combining geology, petrography, and geochemistry, on the rocks of the isolated hill of Mount Calanna (Mount Etna, Italy) has provided evidence for the existence of a dyke swarm, formed by more than 200 dykes distributed over an area of ~ 0.7 km², with an intensity of intrusion up to 40%. All bodies are deeply altered, and the geological and mesostructural surveying of 132 dykes revealed that they intruded in E–W direction, with an average dip of 60°. The faults affecting the outcrop have in general an E–W strike and dip of $\sim 55^\circ$: these have all normal motion and have been interpreted as coeval with the dykes. This interpretation contrasts with the previous hypothesis that considered Mount Calanna as a thrust resulting from compressive deformation resulting from the gravitational spreading of the volcanic edifice. Mount Calanna is here interpreted as the uppermost portion of a vertically extensive magmatic plexus that fed the eruptive activity of one (or more) eruptive center/s sited in the Valle del Bove area. Measurements of the apparent densities on 23 dykes and host rock samples give an average value of 2,420 kg/m³ for the entire complex, $\sim 15\%$ lower than the density expected for hawaiitic magma, placing an important constraint on the geophysical identification of similar structures. Considering

that Mount Etna is not an old eroded edifice but an active and growing volcano, the exposure of this subvolcanic structure can be regarded as exceptional. Its geometry and physical characteristics can be thus regarded as an interesting example of the present-day shallow plumbing system of Mount Etna as well as of other basaltic volcanoes.

Keywords Etna · Shallow plumbing system · Faults · Gravitational spreading · Magma density

Introduction

The study of a volcanic system cannot disregard the way in which magma rises to the surface through the upper crust and the volcanic edifice, that is, its plumbing system. These could develop in several ways, mainly depending on the geodynamic setting of the volcanic area (Gautneb and Gudmundsson 1992; Walker 1992; Rollin et al. 2000; Corsaro and Pompilio 2004b; Klausen 2006; Gudmundsson 2006; Acocella et al. 2006; Porreca et al. 2006). Starting from their source, magmas rise toward the surface and can stagnate at different levels in the lithosphere. In central volcanoes, the uppermost levels of plumbing systems are generally constituted by an articulated network of prevalent vertical or subvertical fractures filled with magma, i.e., dykes. In active volcanoes, plumbing systems are not exposed; therefore, their understanding can be reached only through indirect evidence and analogies. Geophysics can provide information on the geometry of plumbing system, magma chamber/s, mechanisms of emplacement of dykes, etc. (e.g., Murru et al. 1999; Iuliano et al. 2002; De Gori et al. 2005; Mattia et al. 2008), but another way to understand the mechanism of emplacement of dykes swarm is to study subvolcanic bodies (i.e., magma chambers, dykes, and sills), which reside in the upper

Editorial responsibility: R. Cioni

Electronic supplementary material The online version of this article (doi:10.1007/s00445-010-0398-z) contains supplementary material, which is available to authorized users.

C. Ferlito (✉) · E. Nicotra
Dipartimento di Scienze Geologiche, Università di Catania,
Corso Italia 57,
95129 Catania, Italy
e-mail: cferlito@unict.it

E. Nicotra
e-mail: eugenio.nicotra@unict.it

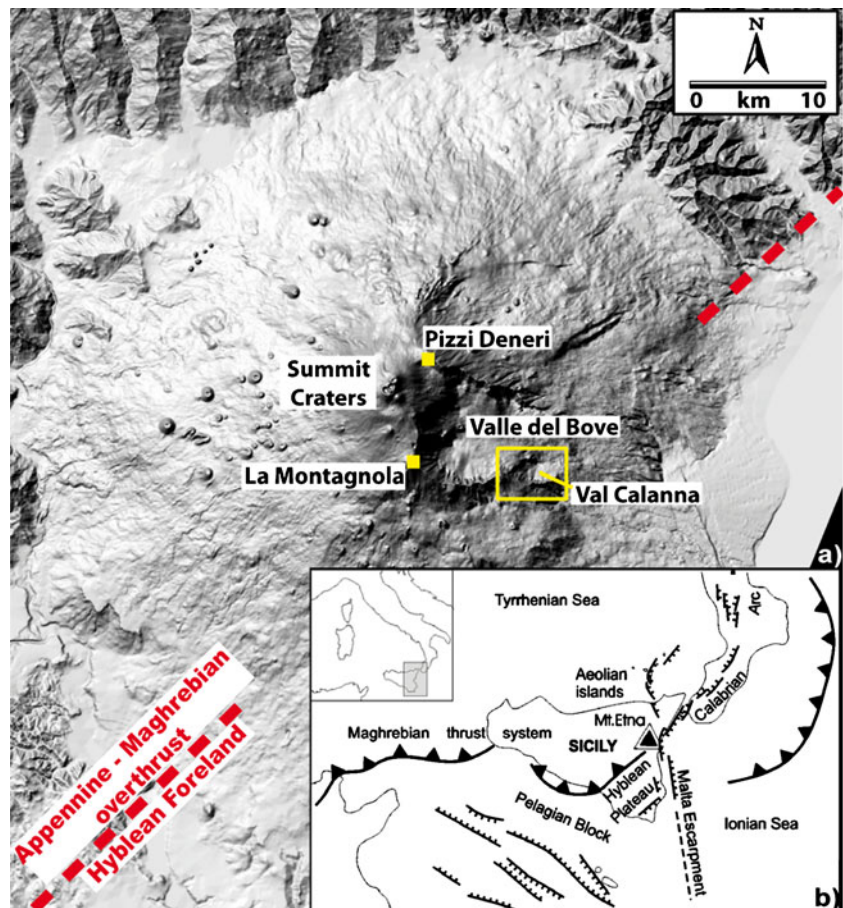
crustal levels and commonly crop out in the deeply eroded roots of many volcanic edifices characterized by basic volcanism. Such subvolcanic structures often provide a substantial amount of information on the feeding system of the volcano as well as on the local and regional stress regime (Gautneb et al. 1989; Jolly and Sanderson 1995; Marinoni and Gudmundsson 2000; Marinoni 2001; Klausen 2004, 2006; Gudmundsson 2006; Porreca et al. 2006; Acocella et al. 2006; Corazzato et al. 2008). Moreover, structural data on the dyke swarms are of great importance for understanding the tectonic evolution of volcanoes, in particular because dyke location and orientation provide important information on the controlling paleostress field at the time of their emplacement (cf. Marinoni and Gudmundsson 2000; Marinoni 2001 and references therein). Furthermore, the study of this intriguing topic could provide paramount constraints for the recognition and tracking of magmatic processes and magma dynamics within the plumbing system and, consequently, the eruptive behavior.

Most of the edifice of present-day Mt. Etna volcano has grown in the last 80 ka, even though the volcanic activity began about 500 ka ago (Romano 1982; Gillot et al. 1994; Coltelli et al. 2000; Catalano et al. 2004; De Beni et al. 2005; Branca et al. 2008). In spite of its “young” age, the

intense erosional regime of the eastern flank of Mt. Etna and, in particular, inside the huge depression of Valle del Bove (Fig. 1) has exposed several subvolcanic bodies (Lanzafame and Vestch 1985; Ferlito and Cristofolini 1989, 1991; Calvari et al. 1994; Coltelli et al. 1994). Most of these bodies are dykes cutting the volcano-stratigraphic succession, whereas other complex subvolcanic structures such as necks or dykes stocks are rare and occur only on the steep western wall of the Valle del Bove (Ferlito and Cristofolini 1991; Calvari et al. 1994). Moreover, magma bodies intruded and solidified at crustal level have recently been identified using seismic tomographies (Hirn et al. 1991; Villaseñor et al. 1998; Laigle et al. 2000; Lombardo et al. 2000; Aloisi et al. 2002), as well as gravimetric and magnetic anomalies (Rollin et al. 2000).

At Mount Calanna (MC), located in the SE area of the Valle del Bove, a great number of dykes have been noticed by several authors (Klerkx 1970; Romano and Sturiale 1975; Romano and Guest 1979; McGuire 1982; Romano 1982; Ferrari et al. 1989). All authors have recognized the importance to this small outcrop, since it represents a portion of the roots of the volcano now exposed by the erosion. However, a systematic study of the dykes and structures has never been done. We have therefore performed a multidis-

Fig. 1 **a** Digital elevation model (DEM) of Mt. Etna (modified after Monaco et al. 2008). The *box* outlines the geographical position of Val Calanna. **b** Sketch map of Mt. Etna showing the regional framework of Southern Italy (modified after Monaco et al. 2005)



ciplinary study to constrain the relationships among the intrusive bodies and to define their physical properties. We propose that the subvolcanic complex recognized at MC could represent an example of the uppermost portion of the Etnean plumbing system. Results obtained provide (1) an alternative volcanological interpretation of MC; (2) a better understanding of the past tectonic regime in the Valle del Bove area and, more in general, of the eastern flank of Mt. Etna; and (3) the physical and geological features of subvolcanic complex at Mt. Etna, also useful to the understanding of similar basaltic volcanoes.

Volcanological background

Mount Etna (eastern Sicily) is a Quaternary composite volcano, which has grown to its present elevation of ~3,340 m a.s.l. by accumulation of lavas and pyroclasts. The volcanic edifice is located between two important regional domains (Fig. 1): the Hyblean Plateau and the Maghrebian thrust system (Lentini 1982; Cristofolini et al. 1979; Ben Avraham and Grasso 1990). The Hyblean Plateau constitutes the southeastern corner of Sicily and is made up of a Meso-Cenozoic carbonatic succession. Mount Etna is at the front of the Maghrebian belt above an early–middle Pleistocene foredeep clayey succession (Wezel 1967; Cristofolini et al. 1979), deposited on the flexed margin of the Hyblean Plateau and containing several levels of tholeiitic and transitional pillow lavas and hyaloclastites dating from 500 to 220 ka (Gillot et al. 1994; Corsaro and Cristofolini 1996; De Beni et al. 2005; Branca et al. 2008). Eastern Sicily was also affected by an intensely extensional tectonic regime associated with the Malta escarpment (Fig. 1b), a NNW–SSE directed system of lithospheric faults that separates the continental crust of eastern Sicily from the

oceanic crust of the Ionian Basin (Finetti 1982; Ben Avraham and Grasso 1990; Hirn et al. 1997).

The Mount Etna edifice is constructed of lavas and pyroclastic deposits with a Na-alkaline character mainly erupted in the last 220 ka (cf. Gillot et al. 1994; De Beni et al. 2005; Branca et al. 2008). The eruptive history of alkaline products is “classically” divided into four major phases, corresponding to four volcano-stratigraphic units (Cristofolini et al. 1979; Romano 1982; Gillot et al. 1994; Catalano et al. 2004; Monaco et al. 2005 and references therein): Ancient Alkaline Centers (AAC; 220–120 ka), Trifoglietto (80–60 ka), Ancient Mongibello (or Ellittico; 60–15 ka), and Recent Mongibello (15 ka to present). Products of Ancient and Recent Mongibello cover ~85% of the present volcano surface (Catalano et al. 2004) and are poorly evolved, mostly hawaiites, with SiO₂ ranging between 48% and 52% (Cristofolini et al. 1991; Tanguy et al. 1997; Corsaro and Pompilio 2004b). Eruptions are mostly effusive and occur through the summit activity and lateral vents usually located along fractures controlled by regional tectonics with most common orientations NNW–SSE, ESE–WNW, WSW–ENE, and NE–SW (Lo Giudice et al. 1982; McGuire and Pullen 1989; Monaco et al. 1997, 2005).

The main morphological feature on the eastern flank of Mount Etna is the Valle del Bove. This is a horseshoe-shaped depression 7 km long, 5 km wide, and 0.8 km in maximum height. The geology of the Valle del Bove has been extensively studied (Romano 1982; Mc Guire 1982; Lanzafame and Vestch 1985; Ferlito and Cristofolini 1989; Calvari et al. 1994, Coltelli et al. 1994, D’Orazio et al. 1997): its floor is covered by very recent lava flows, while the volcanic sequences associated with some important Na-alkaline centers are exposed on its steep walls starting from the AAC to the Mongibello (Figs. 2 and 3).

Fig. 2 Overview of Mount Calanna surrounded by 1991–1993 lava flows. Mt. Etna summit craters in the background

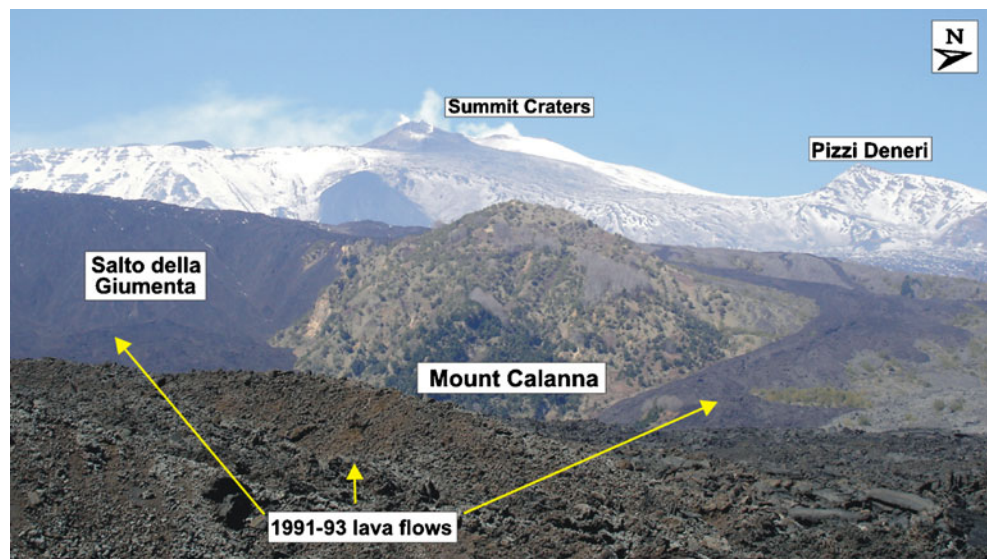
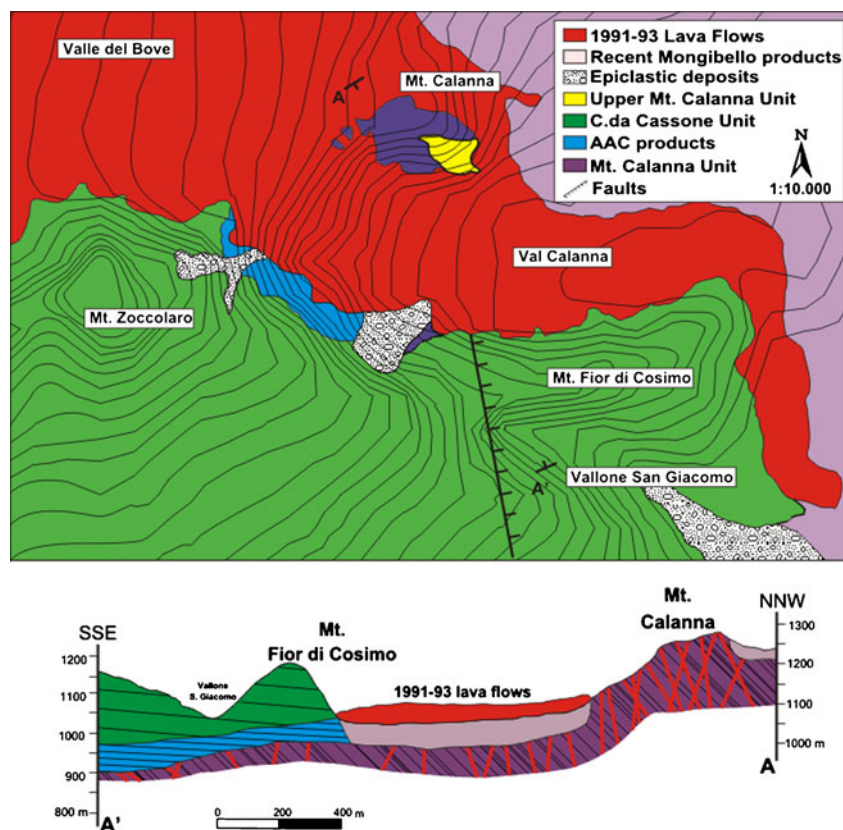


Fig. 3 **a** Geological sketch map of the Val Calanna area. Upper boundaries of the AAC products and those of C.da Cassone Unit are taken and modified after Ferrari et al. (1989). **b** Stratigraphic section along the A–A' profile, legend as in **a**



The 1-km wide and 2-km long depression of Val Calanna is cut at the SE margin of the Valle del Bove and is bordered to the S by the slopes of Mt. Zoccolaro and Mt. Fior di Cosimo (Fig. 3); to the W it is separated from the nearby Valle del Bove by the “Salto della Giumenta,” a steep 300-m high slope, covered by recent lava flows (Fig. 2). On the northern flank, the Val Calanna is bordered by MC, an isolated hill extending over an area of 0.7 km², with a maximum elevation of 1,325 m a.s.l., and surrounded by recent historical lavas (Figs. 2 and 3). The rocks cropping out at MC have attracted the curiosity of researchers working on Mt. Etna. Klerkx (1970) and Romano and Sturiale (1975) recognized the presence of numerous dykes cutting the MC and the lava sequence and a thick cinder layer of the northern slope of Monte Zoccolaro. Romano and Guest (1979) and Romano (1982) pointed out the pervasive alteration of the dykes and the country rock, representing the remnants of an AAC, developed within the present Val Calanna. Later, McGuire (1982) confirmed the stratigraphic position of MC within the AAC, but divided its products in two groups: a first group made up of altered agglomerates and breccias faulted, fractured, and dissected by hawaiitic dikes; a second group constituted by an alternation of scoria and ash beds. On the whole, McGuire (1982) interpreted MC as the neck of a pyroclastic cone intensely intersected by

dykes. Lately, Ferrari et al. (1989) inferred the presence of low angle reverse faults on the southern slope of MC and interpreted the entirety of MC as tectonic thrusts piled up by a compressive tectonic regime. To explain the origin of the compression, they suggested two alternative interpretations: (a) MC represents a portion of the pre-Etnean basement involved in the regional orogenesis or (b) MC is a remnant of the early Etnean edifice deformed by the gravitational spreading. This second interpretation offered support to the model of Borgia et al. (1992), who proposed a gravitational spreading of the eastern flank of Mount Etna. Attempts at absolute dating of the rocks of MC provided unreliable results due to the deep alteration of its products (Ferrari et al. 1989; Gillot et al. 1994). Recently, Branca et al. (2008) have presented a new ⁴⁰Ar/³⁹Ar dating for the rocks in the Val Calanna area, finding an age of 128.7±3.8 for the rocks belonging to MC and an age of 93.0±3.0 ka for the rocks that directly overlie MC.

Sampling and analytical methods

The geological survey was focused on the products of MC and their relationship with the overlying units (Fig. 3). Due to the inaccessibility of some areas, not all dykes and

structures of MC have been surveyed, and a total of 131 measurements of GPS position, strike, and dip were obtained (Table 1 and ESM 1). All measurements have been plotted with GEORIENT 9.4 software (Holcombe-Coughlin and Associates 2008).

Petrochemical and physical data on MC volcanics were collected for 38 representative rock specimens. Whole-rock major element compositions of 19 selected samples were analyzed on powder pellets at the Dipartimento di Scienze Geologiche of the University of Catania (Italy) using a Philips PW2404 WD-XRF spectrometer, with corrections of the matrix effects (Franzini et al. 1972); FeO concentrations were obtained by classic $KMnO_4$ titration. Loss on ignition (LOI), corrected for Fe^{2+} oxidation, was determined by gravimetric methods.

Scanning electron microscopy-energy dispersive spectroscopy (SEM-EDS) analyses on mineralogical phases on ten selected thin polished sections were performed at the Dipartimento di Scienze Geologiche of Catania (Italy) using a Tescan Vega LMU scanning electron microscope equipped with an EDAX Neptune XM4-60 micro-analyzer characterized by an ultra-thin Be window. Analyses were performed at 20 kV accelerating voltage and 0.2 nA beam current. Precision of collected data is on the order of 5%.

Measurements of density were performed on 19 specimens of dykes and four of the host rock. Density was measured on rock cubes with edge of 4.5 cm, dried in oven at 50°C for 72 h. The dried cubes were weighed using an analytical balance. Before measuring their volume, cubes were saturated by immersion in bi-distilled water for 72 h. The volume was measured calculating the Archimedes' force acting on the cube when suspended inside a beaker filled with bi-distilled water. The precision of the method was verified by repeating three measurements on three cubes of the samples labeled as MC1 and MC6. Error was within $\pm 0.02 \text{ kg/m}^3$.

Data results

Geological survey

Rocks cropping out at MC correspond to the Basal Unit of MC, as defined by Ferrari et al. (1989), and are here informally defined as MC Unit. They represent the most ancient formation of the surveyed area (Fig. 3). This unit constitutes the framework of MC and crops out on the southern flank of Val Calanna (below Mount Fior di Cosimo, Fig. 3), where it is covered by lava flows of the ancient eruptive centers, now totally extinct and dissected (cf. Branca et al. 2008; Fig. 3). The lateral extent of the MC Unit is very difficult to estimate; however, rocks having similar features have been found in a groundwater drainage

Table 1 Major elements compositions of Mount Calanna rocks

Sample type	MC 1		MC 3		MC 5		MC 6		MC 8		MC 9		MC 11		MC 14		MC 15		MC 16		MC 17		MC 18		MC 24		MC 27		MC 29		MC 30		MC 31		MC 37					
	AD	AD	AD	AD	AD	AD	AD	AD	AD	UD	HR	AD	AD	UD	UD	AD	UD	UD	UD	AD	AD	AD	AD	HR	UD	AD	AD	AD	AD	AD	AD	AD	AD	AD	AD					
SiO ₂	48.12	48.24	45.82	47.79	46.68	51.44	47.71	47.24	48.50	51.82	50.64	50.80	52.31	50.37	48.77	49.26	50.90	50.99	50.29																					
TiO ₂	1.82	2.25	1.85	1.93	2.11	1.76	1.54	1.93	1.65	1.40	1.66	1.66	1.62	1.66	1.87	2.17	1.86	1.75	1.79																					
Al ₂ O ₃	17.61	16.86	16.78	18.24	18.88	20.45	18.61	17.37	18.17	19.97	19.64	18.81	17.76	19.49	20.16	17.04	17.63	19.14	18.71																					
Fe ₂ O ₃	9.24	11.80	10.77	9.98	12.81	7.14	8.17	10.19	10.05	8.40	8.48	9.03	9.49	8.58	8.70	10.20	9.87	8.05	10.18																					
FeO	3.23	1.01	3.02	5.27	1.41	3.25	2.57	2.56	1.01	3.51	5.07	2.63	1.22	5.25	1.00	2.36	2.16	3.51	0.65																					
FeO _{tot}	11.54	11.63	12.71	14.25	12.93	9.68	9.92	12.01	10.58	11.29	12.76	10.93	10.06	13.02	9.34	11.89	11.34	10.91	10.27																					
MnO	0.16	0.08	0.17	0.16	0.17	0.11	0.14	0.16	0.21	0.14	0.14	0.22	0.13	0.15	0.08	0.14	0.14	0.13	0.13																					
MgO	3.68	5.81	5.04	4.14	3.65	1.61	4.05	6.38	6.03	1.49	2.16	1.82	3.89	2.27	4.03	4.11	3.67	2.01	3.39																					
CaO	8.47	3.31	7.50	9.13	5.46	7.98	6.99	8.15	4.88	7.71	8.46	8.45	4.64	8.62	4.88	7.20	6.31	8.65	6.33																					
Na ₂ O	3.83	4.04	4.69	4.22	4.09	3.93	5.15	3.49	2.92	3.98	5.05	4.22	4.36	5.18	3.29	3.28	3.96	4.18	3.05																					
K ₂ O	1.77	0.17	1.02	1.54	0.55	2.31	1.79	1.01	1.50	1.51	2.08	2.02	1.76	2.08	1.50	1.86	1.71	2.09	0.58																					
P ₂ O ₅	1.01	0.78	0.64	0.80	1.32	1.02	0.62	1.14	0.64	0.84	1.04	0.97	0.68	1.02	0.63	1.01	0.70	0.97	0.73																					
LOI	4.28	6.64	5.72	2.08	4.29	2.26	5.23	2.93	5.46	2.74	0.66	2.01	3.36	0.58	6.09	3.72	3.27	2.04	4.82																					

AD altered dykes, UD unaltered dykes, HR host rock

gallery located ~1.5 km southward of Val Calanna (cf. Branca et al. 2004). The eastern portion of MC is covered by a 40-m thick sequence of porphyritic hawaiitic lava issued from a more recent dyke cutting the MC Unit and oriented 210°N, probably best ascribed to the Mongibello volcanic phase. This formation is here informally defined as Upper MC Unit and fully corresponds to the “Unità Superiore di Val Calanna” of Ferrari et al. (1989). To the north and west, the MC Unit is covered by the lava flows of recent Mongibello and, in particular, by those of the 1991–1993 eruption (Figs. 2 and 3).

The geological survey revealed that the frame of MC is composed of a considerable number of dykes intruded into a deeply altered host rock. A total of 200 dykes was counted over an area of about 0.7 km²; however, the vegetated and crumbly slopes have prevented us from measuring strike and dip angles for all of them. Dykes crop out on the entire MC hill, although they are more concentrated on its southern flank. The intensity of intrusion of dykes, defined by Walker (1992) as the ratio between the volume of dykes intruded and the total volume, has been estimated at about 40%. Dykes that crop out on MC display a broad range of macro- and mesoscopic features. An evident characteristic of these dykes is the highly variable alteration, from fresh unaltered to deeply altered bodies.

Altered dykes (AD; Fig. 4) constitute most of the studied dykes (~90%), presenting the highest intensity of intrusion (up to 60%) on the southern flank of MC. AD show a yellow-brownish color on the external surfaces and a lilac color along the fracture surfaces (Fig. 4b). They are cut by a dense fracture network that often masks the original aspect

of the dykes (Fig. 4b). Many AD have thickness ranging between 0.4 and 2 m. On the southern flank of MC, several thin (0.3–0.4 m) dykes are joined together to form compound bodies 15–20 m thick, thus testifying multiple injection events along the same plane. AD are generally vesicular, with bubbles up to 5 mm in diameter.

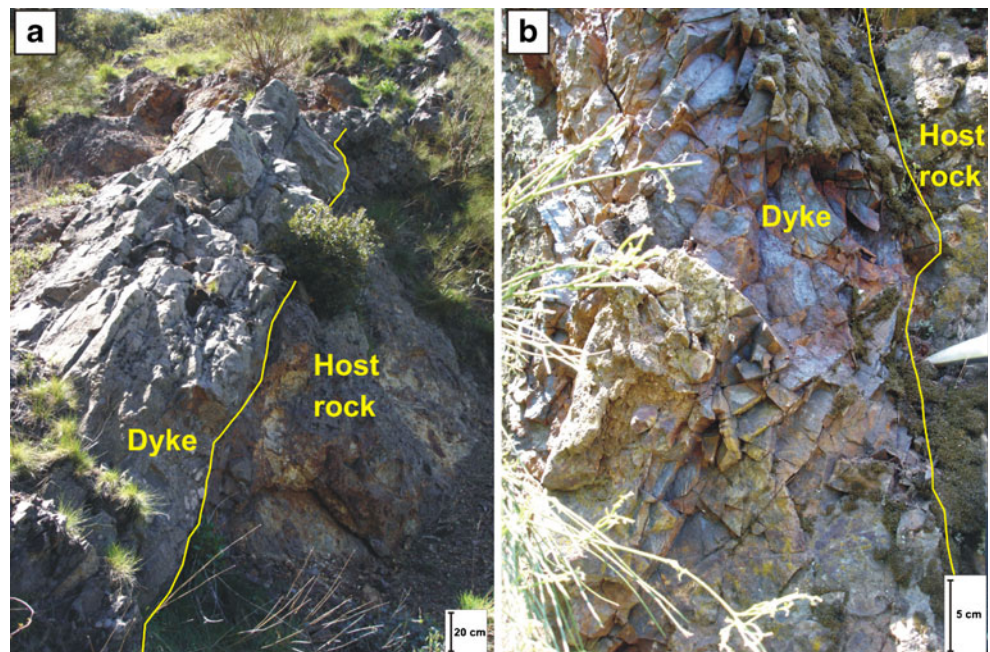
Unaltered dykes (UD) were also observed on MC (Fig. 5), often cutting both the AD and the faults. These dykes were also observed and described by Ferrari et al. (1989), who interpreted them as the feeders of subsequent eruptive events on the Val Calanna area. Their thickness ranges between 1 and 3 m and, commonly, they have chilled margins and vesicles up to 4 mm.

Host rock is deeply altered, often making it difficult to recognize the original lithology. It exhibits yellow-brownish aureoles of alteration, which initiate from the dykes where the coloration is more intense (Fig. 4). In the southern flank of MC, where the highest concentration of dykes occurs, the host rock comprises an intensely altered breccia yellowish in color (Fig. 4). In areas less affected by the intrusion of dykes, like the northern and eastern flanks of MC, the breccia has a predominantly brownish color, and it is possible to recognize some vesicular dark gray breccias and blocks with visible crystals of plagioclase; these features allow us to interpret the host rock of MC as volcanic products (lavas and/or pyroclastic deposits).

Mesostructural survey

Dykes and host rock are both affected by strong development of tectonic faults and joints. Twenty-six faults have been

Fig. 4 The altered dykes (AD) of Mount Calanna. **a** Altered dyke on the eastern flank of MC; the *yellow line* evidences the boundary with the host rock. **b** Altered dyke on the southern flank of Val Calanna and its boundary with the host rock; the dyke shows intense fracturing and a local color of alteration along the surfaces of the fractures



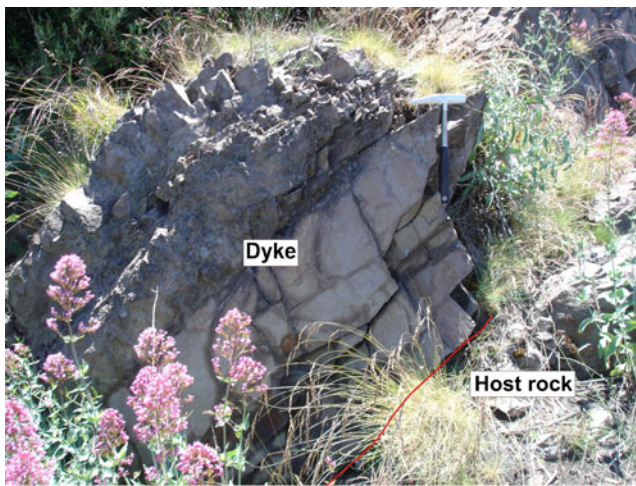


Fig. 5 Unaltered dyke (UD) cropping out on the northern flank of Mount Calanna and its contact with the host rock (see text for description)

surveyed in 0.7 km² of MC, and their strike and dip are reported in ESM 1. On the southern flank of MC, faults are often associated with cataclastic bands as thick as ~40 cm (Fig. 6); their breccias and the associated matrix are often deeply altered, with bands of yellowish alteration. Structural

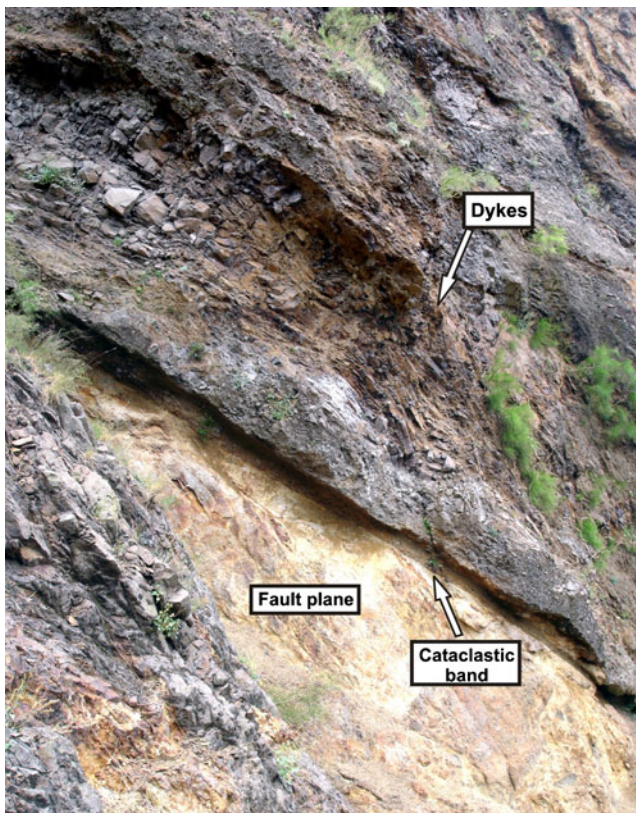


Fig. 6 Fault in the SW flank of Mount Calanna. Above the fault plane, a 30-cm thick cataclastic band is visible (see text for description)

survey of the faults has shown as all of them present on their planes marked fault steps (Fig. 7): these structures, typical indicators of the sense of motion of faults, have the steepest flank on their lower side, suggesting a downward movement of the hanging wall with respect to the footwall. Often, fault traces are not straight but slightly folded with an “opening angle” of ~120°. Offsets along the faults have not been determined because no features can be correlated from the hanging wall to the footwall. Cross-cutting relationships between faults and AD are absent (high degree of parallelism), whereas the UD cut both faults and the AD. Furthermore, a great number of joints, cutting dykes, host rock, and also faults displacing MC in several blocks have been surveyed. These are often open (3–5 cm), and only on 20% of them alteration surfaces were found, all associated with the AD.

In a previous survey, Ferrari et al. (1989) described two outcrops on the southern flank of MC and interpreted them as providing evidence of ramp structures to low angle faults associated with a compressional regime. This interpretation had a paramount role in a further work, in which it was envisaged that the volcanic edifice of Mount Etna was undergoing gravitational spreading, which produced compressive structures at its periphery (Borgia et al. 1992). In our survey, we carefully re-examined the same outcrops on the southern face of MC, without finding any clear evidence of ramps or other compressional structures. On the contrary, all structures affecting MC are tensile. We suggest that Ferrari et al. (1989) may have possibly misinterpreted niches, formed by erosion acting along planes between adjacent dykes, as portions of compressive ramps.

Faults and joints affecting the AD and UD (Fig. 8) show the greatest consistency (Rose diagram) of structures and their density pole distributions. The AD include about 90%

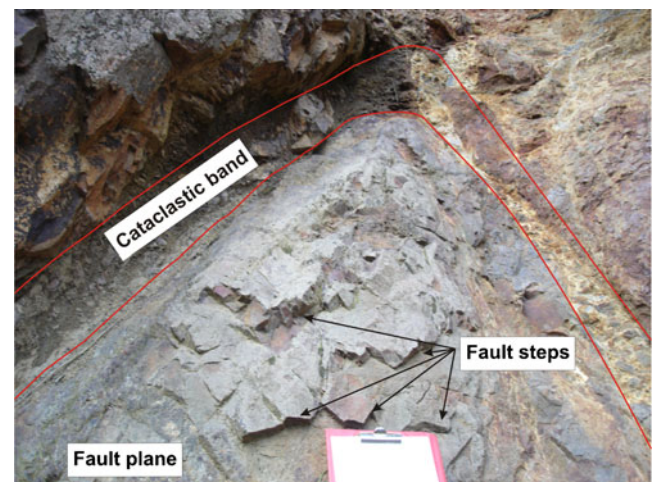
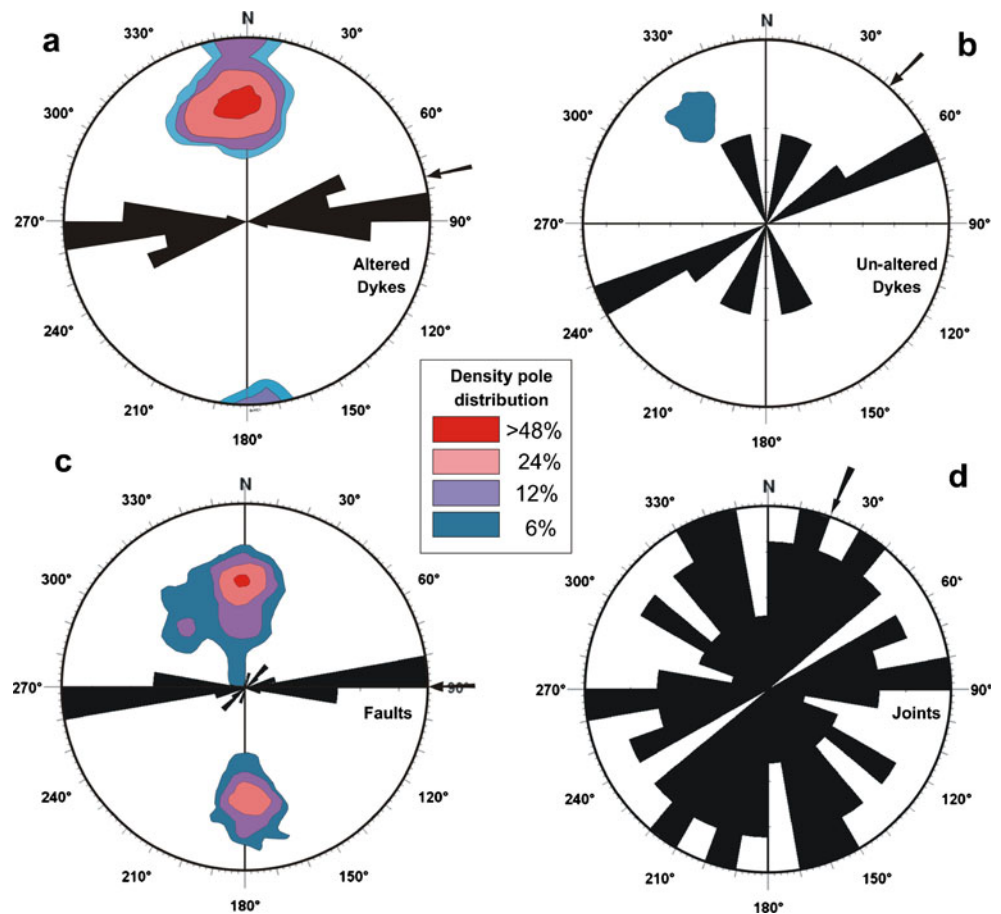


Fig. 7 Fault plane in the southern flank of Mount Calanna with 25 cm of cataclastic band above it. The fault steps are evidenced in the picture which suggest a normal motion of the two fault blocks

Fig. 8 Rose diagrams and density pole distribution clouds of dykes, faults, and joints. **a** Altered dykes fit with a most frequent strike of intrusion 83°N; the strike corresponds to the 83°N oriented and 60° inclined plane perpendicular to the pole with the highest value of density distribution (>46%). **b** Unaltered dykes do not show a clear strike of intrusion, having a density pole distribution of less than 15%. **c** Faults have similar direction of AD, with 90°N of direction and 60° of dip angle; they show a conjugate system with planes dipping towards N and S. **d** Joints are very scattered and do not show any relevant principal direction



of the MC dykes. Their most frequent strike is 83°N, with dips ranging between 50° and 90° (Fig. 8a). The density poles distribution shows homogeneous values of strike and dip for the AD, with values of density higher than 46% for a plane striking 83°N and 60° of dip. Strikes and density pole distribution of UD are less homogeneous (~10% value of density; Fig. 8b); however, a prevalent NE–SW strike can be noticed. Faults display most frequent strike of 90°N, with the dip ranging of 50–65° (Fig. 8c). The density pole distribution (Fig. 8c) indicates that the most common orientation is 90°N with dip of 55°. Dip directions are both N and S, as expected by conjugated systems of normal faults. Joints have a scattered distribution across the full azimuth range (Fig. 8d). Only a minority can be associated to the tectonic directions common in the Etnean area (see “Volcanological background” section).

Petrography and mineral chemistry

Rocks of the AD are oligophyric to mesophyric with a seriate texture and porphyricity index (PI in volume percent), ranging between 2 and 15. Extreme values have been found for samples MC33 (PI 2) and MC7, MC17, and MC21 (PI 15). Among the phenocrysts, plagioclase (~8 vol.%) and clinopyroxene (~4 vol.%) are the most abundant, followed by minor

olivine (~2 vol.%) and opaque oxides (~1 vol.%). In addition, amygdales commonly occur in all the observed rocks (Fig. 9b). Groundmass ranges from hyalopilitic to intersertal with brownish altered glass joined to microlites of plagioclase, clinopyroxene, and opaque oxides. Vesicles are widely present in all AD, with ellipsoidal bubbles ranging in size between 1 and 5 mm. Plagioclase phenocrysts vary in size between 1 and 5 mm, with subhedral to anhedral habitus. All phenocrysts are fractured, with brownish clay minerals filling fractures and partially or totally substituting the crystal structure (Figs. 9a and 10a). In order to have a characterization of plagioclase, major oxides analyses have been performed on their cores and are reported together with structural formulae calculated on the basis of five cations and eight oxygens (ESM 1). On the whole, compositions range between labradorite and bytownite, with a high frequency of An_{75–85} (mole percent; Fig. 11a and ESM 1); such compositions are comparable with those found by Nazzareni et al. (2003) for AAC clinopyroxenes. Clinopyroxene occurs only in a few samples of AD and euhedral to subhedral crystals with medium (0.5–2 mm) size. They are often fractured (Fig. 10b), although to a lesser extent than plagioclase, and they show optical zoning and pale-green color (Fig. 9), typical of the Etnean clinopyroxenes (Nazzareni et al. 2003). Major oxide analyses were

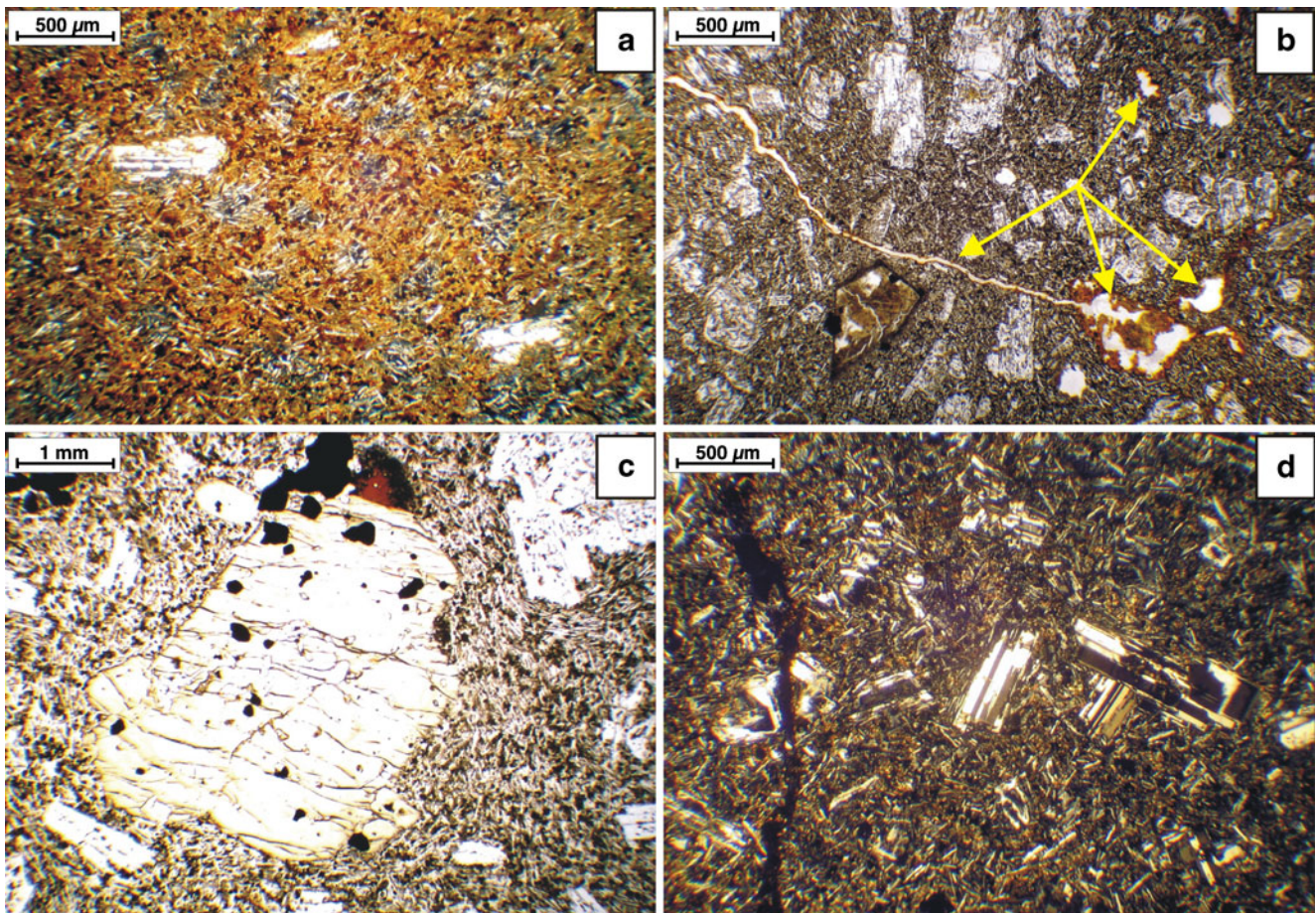


Fig. 9 Polarized microscopy images of dykes and host rock of Mount Calanna. **a** Altered dyke (AD); the texture is oligophyric with phenocrysts of plagioclase in an intersertal and altered groundmass (*plane polarized light*). **b** AD with a deep alteration of groundmass and phenocrysts (*cross polarized light*; see text for description); *yellow arrows* point toward secondary minerals that fill fractures and cavity

in the rock (i.e., amygdales). **c** Unaltered dyke with phenocrysts of plagioclase, clinopyroxene, olivine, amphibole, and opaque oxides in a pilotassitic groundmass (*plane polarized light*; see text for description). **d** Host rock with plagioclase phenocrysts in an intersertal groundmass (*cross polarized light*; see text for description)

performed on the cores of clinopyroxene crystals, with measured compositions reported together with structural formulae calculated on basis of four cations and six oxygens in ESM 1. On the QUAD diagram, compositions range across the full range of the diopside and augite fields (Fig. 11b). Following the classification of Morimoto et al. (1998), AD pyroxenes can be classified as “Ti-bearing” Al-Fe³⁺-augite and Al-Fe³⁺-diopside, with values similar to those found by Nazzareni et al. (2003) for AAC pyroxenes. Olivine occurs as rare anhedral small phenocrysts (0.2–1 mm), with frequent iddingsitic alterations on their rims or sometimes through the entire crystal (Figs. 9b and 10c). Due to alteration, only a few major oxides analysis have been performed (ESM 1), showing a constant composition of Fo₇₅ (mole percent; Fig. 11c and ESM 1) similar to the AAC olivines (Nazzareni et al. 2003). Oxides are present as phenocrysts and in the groundmass as euhedral to subhedral crystals of small size (<1 mm); oxides frequently occur inside and/or together with olivine and clinopyroxene phenocrysts, suggesting an early

stage crystallization. Major element analyses allowed us to recognize opaque oxides as Ti-magnetite (Fig. 11d and ESM 1). The most important petrographic feature of the AD is the deep alteration that affects phenocrysts (Figs. 9 and 10) and groundmass. Secondary minerals, red-brownish in color, fill vesicles and fractures (Fig. 9a, b). Microlites of plagioclase and opaque oxides of the groundmass are extensively affected by alteration (Fig. 9a, b), resulting in a very intense yellow-brownish coloration.

Rocks of the UD are mesophyric with seriate crystal textures and PI ranging between 20 and 30 (Fig. 9c). Major element oxides have been measured by means of SEM-EDS, and data along with structural formulae calculations are reported in ESM 1. Among the phenocrysts, An_{60–78} plagioclase (~15 vol.%) and augitic clinopyroxene (~10 vol.%) are the most abundant, followed by Fo_{72–76} olivine (~3 vol.%), opaque oxides (~2 vol.%), and amphibole (~1 vol.% in the MC8 and MC16 samples; Fig. 11). Although their compositions are similar to those of

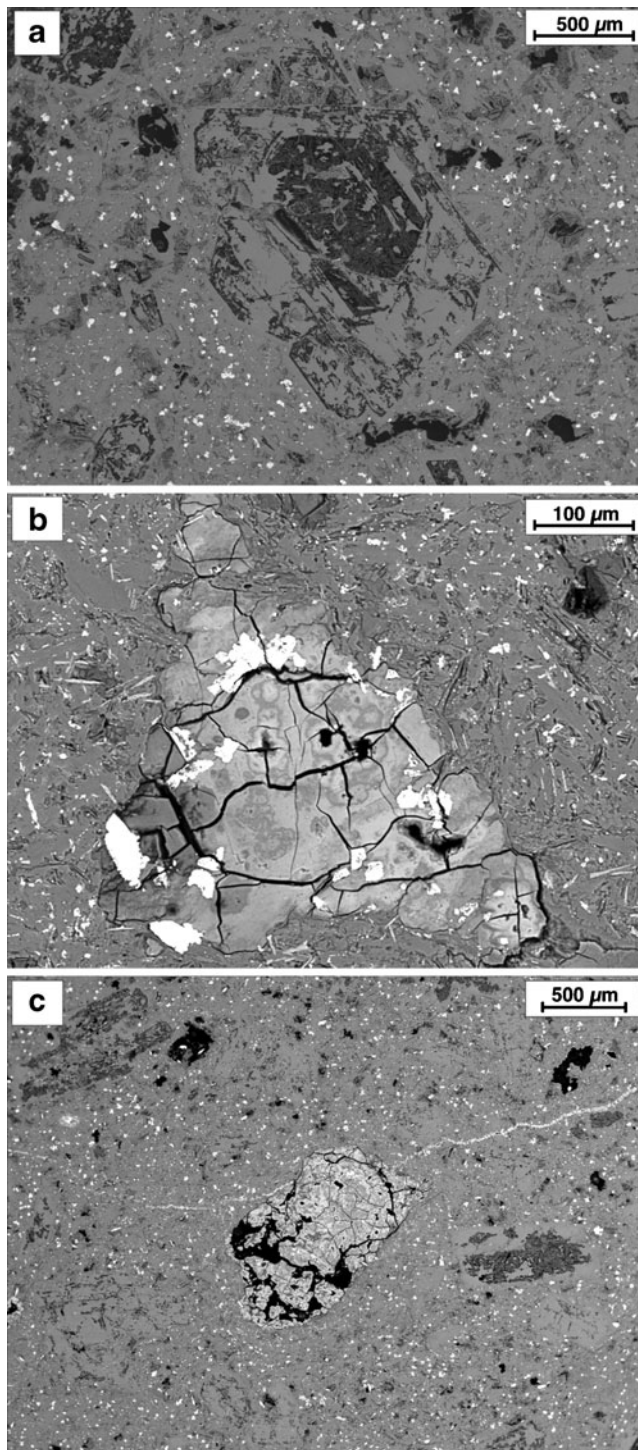


Fig. 10 Compositional variation of the mineral phases of Mount Calanna volcanics: (a) plagioclase crystals, (b) clinopyroxene crystals, (c) olivine crystals, and (d) opaque oxides

the typical Etnean volcanics, a comparison with the dataset of the AAC of Nazzareni et al. (2003) reveals that the UD phenocrysts have a more evolved signature. The groundmass varies from hyalopilitic to intersertal with variable

amounts of glass and microlites of plagioclase, clinopyroxene, subordinate olivine, and opaque oxides. Glomerophyritic structures also occur, with aggregates of clinopyroxene, olivine, and oxides. The UD lack alteration and fracturing of phenocrysts and groundmass (Fig. 9c).

The rocks hosting the dykes (HR) of MC are oligophyric with a seriate texture and a PI ranging between 5 and 10 (Fig. 9d). The mineral assemblage is typical of Etnean volcanics, with plagioclase (~8 vol.%), clinopyroxene

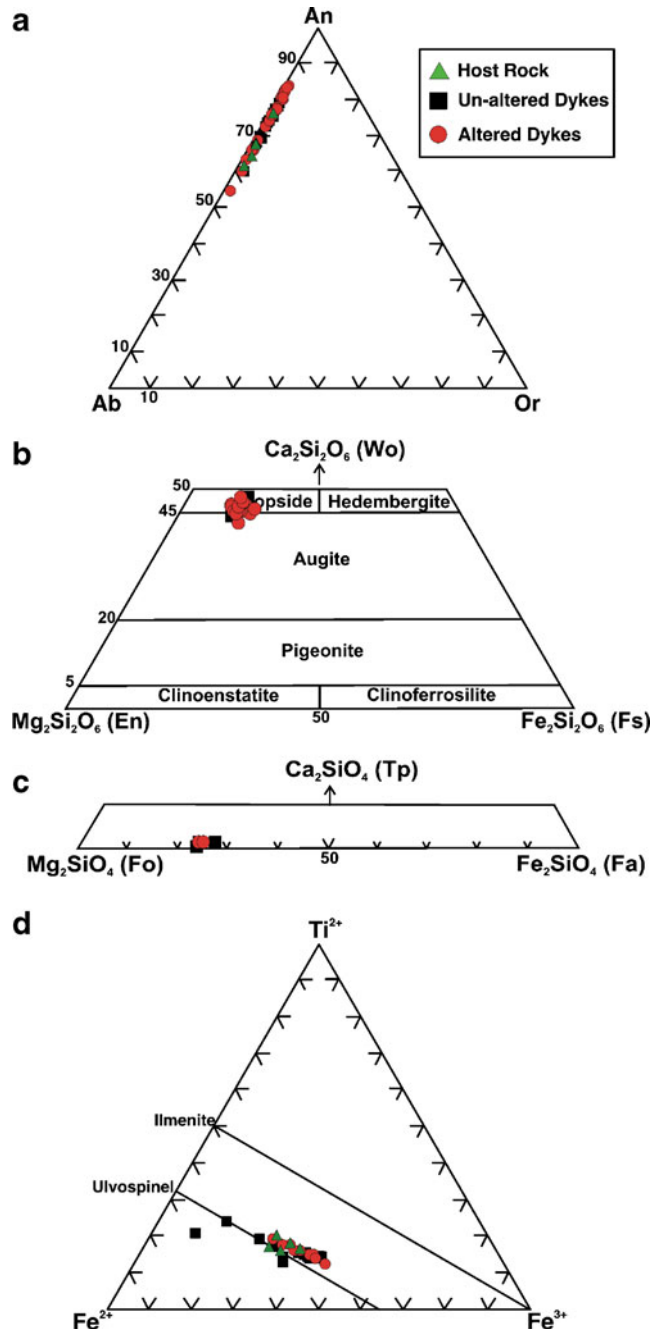


Fig. 11 Backscattered electron images of altered phenocrysts in the Mount Calanna volcanics: (a) plagioclase, (b) clinopyroxene, and (c) olivine

(~2 vol.%), olivine (~2 vol.%), and opaque oxides (~1 vol.%; Fig. 9d). Groundmass is intersertal with variable amounts in volume of brownish glass and microlites of plagioclase, olivine, and opaque oxides. Vesicles are common in these rocks. All phenocrysts are deeply fractured and altered, with brownish secondary minerals that fill the fractures (Fig. 9d). Their crystalline structure is often partially or totally destroyed by the alteration, with secondary opaque and brownish microlites. Due to this high degree of alteration, only one sample was suitable for an SEM-EDS study of major oxides, analyzing only plagioclase and oxides phenocrysts (ESM 1). Plagioclase varies in size between 2 and 4 mm, with habitus from euhedral to anhedral; compositions range between labradoritic and bytownitic terms, with a wide range of An (mole percent) content, being An_{61-76} (Fig. 11a and ESM 1). Clinopyroxene is present only as relicts of phenocrysts, with the crystal structure completely altered. Olivine occurs as anhedral microphenocrysts (0.1–0.8 mm); all crystals have iddingsitic alteration that affects most of the crystal structure, turning the crystals brownish in thin section. The ubiquitous opaque oxides occur as phenocrysts and in the groundmass as euhedral to subhedral crystals with small grain size (<1 mm); major element analyses allowed us to define oxide crystals as Ti-magnetite (Fig. 11d and ESM 1). In general, HR are deeply altered, with secondary minerals that partially or totally fill the vesicles and the fractures; these minerals display very similar features to those of AD. Groundmass is extensively affected by the alteration, evidenced by a very intense yellow-brownish color of glass, plagioclase microlites and opaque oxides (Fig. 9d).

Whole-rock geochemistry

The high degree of alteration of the rocks of MC, shown by macro- and microscopic observation (Figs. 9 and 10), makes problematic the use of geochemical data to characterize products of the MC Unit. Indeed, both the AD and HR show a loss on ignition (LOI) up to 6% (Table 1) that does not allow a geochemical classification for many of the sampled products by using the Total Alkali Silica (TAS) diagram (Le Maitre 2002). Following the IUGS recommendations for classification of volcanic rocks (Le Maitre 2002), it was possible to plot on the TAS only seven samples (Fig. 12). This diagram shows that the dykes of MC can certainly be attributed to the Na-alkaline suite of the Etnean succession (cf. Tanguy et al. 1997), falling in the hawaiitic-mugearitic fields, whilst the host rocks fall in the field of basalts. Major elements composition (Table 1 and Fig. 12b, c) does not reveal any correlation, neither among lithotypes nor between AD and UD. On the whole, the AD show a wide range of SiO_2 (48.5–54.1 wt.%), MgO (1.65–2.37 wt.%), CaO (3.55–8.40 wt.%), and K_2O (0.18–2.36 wt.%; Table 1); whilst the Si and Mg contents can be plotted along a liquid line of

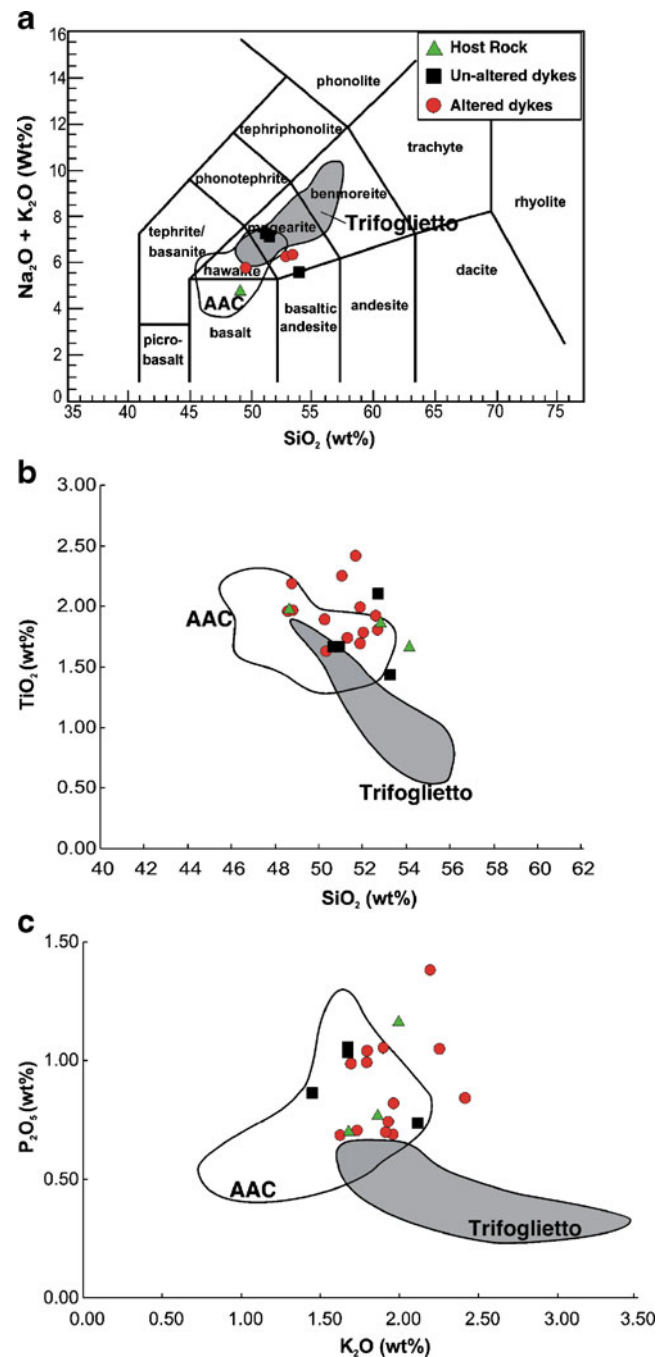


Fig. 12 a Total alkali silica (TAS) diagram (Le Maitre 2002) for volcanics of Mount Calanna. Following the IUGS recommendations, only samples having LOI <2 wt.% have been plotted. b, c SiO_2 vs. TiO_2 and K_2O vs. P_2O_5 diagrams for the volcanics of Mount Calanna; compositional fields of the AAC and the Trifoglietto eruptive centers are plotted for comparison (data from Cristofolini et al. 1991 and references therein)

descent, samples having the same degree of differentiation present very scattered CaO and K_2O compositions which cannot be explained with a simple differentiation process; it must result from alteration. In contrast, TiO_2 , FeO_{tot} , and Na_2O present only small differences, depending on the

degree of evolution of magma. The compositional fields of the AAC and Trifoglietto volcanics (Cristofolini et al. 1991 and references therein) have been plotted for comparison (Fig. 12b, c) together with the Calanna rocks. Most of the AD compositions show high values of TiO_2 and P_2O_5 , plotting into the field of the AAC.

Whole-rock composition of the HR of the MC Unit shows a wide degree of evolution in magma (SiO_2 and MgO , respectively, ranging 48.7–54.1 and 3.56–6.58 wt.%; Table 1), which matches with the typical Etnean range (cf. Cristofolini et al. 1991; Fig. 12). However, no further consideration of the major elements compositions of these rocks is merited, because it was possible to analyze only few samples where, in turn, results are deeply altered, with values of LOI up to 3.36 wt.% (Table 1).

The UD show the same compositional range as the AD, though with a smaller compositional range (Table 1 and Fig. 12). The most noticeable geochemical feature of these dykes is that although they did not show visible alteration, some of them present high values of LOI (up to 2.6 wt.%) and $\text{Fe}_2\text{O}_3/\text{FeO} > 1$, suggesting that weathering affected these rocks, slightly changing their original chemical composition.

Density of dykes and host rock

Apparent density of AD, UD, and of the host rock is shown in Table 2. AD show a broad range of values between 2,050 and 2,810 kg/m^3 (average value of 2,460 kg/m^3) for the 19 measured rock cubes. In spite of the broad range of density, most of the samples have densities lower than the typical value for basaltic rocks of 2,800 kg/m^3 (Corsaro and Pompilio 2004a). Only two UD samples have been measured, with values of apparent density of 2,700 and 2,720 kg/m^3 , consistent with the minor alteration of these dykes and their lower vesicularity. The apparent density of the host rocks has been measured in four samples, with values ranging from 2,330 to 2,490 kg/m^3 , very close to the apparent density assumed in literature for lavas and pyroclastic products (Corsaro and Pompilio 2004a).

Discussion

Mount Calanna: an emerging dyke swarm at Mount Etna

The isolated hill of MC, in spite of its limited size, acquired a notable interest within the scientific community when it was mentioned as one significant proof of the gravitational spreading of the eastern flank of Mount Etna under its own weight (Borgia et al. 1992). Such a conclusion has been put forward based on the hypothesis of Ferrari et al. (1989), who interpreted MC as a set of piled up thrusts. The structural survey presented here does not support the presence of

Table 2 Density values of the rocks of Mount Calanna

Sample	Density (kg/m^3)
Altered dykes	
MC1 (1)	2.59
MC1 (2)	2.61
MC2	2.64
MC5	2.39
MC6 (1)	2.81
MC6 (2)	2.81
MC6 (3)	2.80
MC7	2.17
MC12	2.08
MC17	2.26
MC20	2.42
MC21	2.49
MC22	2.25
MC23	2.66
MC24	2.73
MC31	2.48
MC34	2.19
MC36	2.34
MC38	2.05
Average	2.46
Unaltered dykes	
MC16	2.70
MC8	2.72
Average	2.71
Host rock	
MC18	2.33
MC11	2.35
MC37	2.41
MC30	2.49
Average	2.40

compressional structures. In our interpretation, all faults and joints at MC are related to a tensile tectonic regime with a N–S maximum direction of extension (see below). This would be enough to induce reasonable doubt in considering MC's structural features as a proof of the gravitational spreading of Etna. However, another consideration must also be added: gravitational spreading of volcanic edifices is possible only for edifices with a considerable volume (cf. Merle and Borgia 1996 and references therein). The volume of the volcanic pile of Mount Etna is 374 km^3 , 66% of which was erupted after 80 ka (Catalano et al. 2004). The remaining 34% is not concentrated in one single edifice but is distributed into several small centers scattered over a wide area from the Ionian coast to the northern sector of the present-day edifice (Romano 1982; Catalano et al. 2004; Branca et al. 2008). The absolute age date for MC products is 128 ka (Branca et al. 2008), whereas the lava flows at the base of Mt. Fior di Cosimo that directly overlie the exhumed

products of MC is ~ 95 ka (Gillot et al. 1994; Branca et al. 2008). This suggests that at ~ 95 ka, during the emplacement of the Ancient Alkaline Centers, there was not a large-volume edifice that could produce the significant gravitational spreading, and hence not able to cause compressional tectonics at its base.

At MC the great number of dykes, more than 200, cutting the host rock over an area of 0.7 km^2 , suggests consideration of the MC Unit as a dyke swarm. Most of the swarm consists of AD, with the UD only a minor portion; all cut the AD and therefore predate the emplacement of the main part of the dyke swarm. The AD show relatively homogeneous characteristics (common E–W orientation, similar degree of alteration, low PI, similar mineral assemblage): these allow us to consider their intrusion as having occurred within a constant tectonic regime and probably over a restricted period of time.

Due to the rarity of the outcrops and to their high degree of alteration, the stratigraphic correlations and the evolution of the volcanism, from the beginning of the alkaline phase (~ 220 ka; Gillot et al. 1994; Branca et al. 2008) up to the first central edifices (~ 80 ka; Gillot et al. 1994), are not well understood. This led several authors to group all the eruptive centers into the Unit of Ancient Alkaline Centers (Cristofolini et al. 1979; Romano 1982; Gillot et al. 1994; Catalano et al. 2004) or to the Timpe and Valle del Bove phases (cf. Branca et al. 2004, 2008). The absolute dating and the stratigraphic position of the MC Unit, deduced from the relationships with the overlying volcanic rocks, suggest that the dykes possibly fed one or more Ancient Alkaline Centers. Nonetheless, no certain correlation can be established with formations cropping out in the Valle del Bove or in the nearby area (e.g., Rocche and Tarderìa; cf. Lopez et al. 2006; Branca et al. 2008). More than the absolute dating, whole-rock geochemistry and mineral chemistry suggest an attribution to the AAC for the dykes of MC. In particular, major element compositions of the AD, which represent the framework of MC, have TiO_2 contents too high for correlation of these rocks with the Trifoglietto eruptive center, which is characterized by low TiO_2 contents due to the amphibole crystallization (cf. Cristofolini et al. 1991 and references therein). The high TiO_2 and P_2O_5 contents (Fig. 12b, c) of the AD indicate that these dykes can be ascribed to the AAC phase. UD rocks are certainly younger than to the AAC eruptive phase and present high TiO_2 and P_2O_5 contents (Fig. 12b, c) which, together to their “freshness,” indicate that they belong to the recent Mongibello volcanic phase (cf. Cristofolini et al. 1991; Corsaro and Cristofolini 1996). With respect to the HR, major element compositions (Fig. 12b, c) suggest an attribution of these products to the AAC: however, all that can be conclusively said is that they are older than the MC Unit.

Dyke swarms are interpreted in literature as relevant portions of the plumbing system, and an important element

of a volcano, which represents the conjunction between deep magma storage sites and the volcanic edifice. A plumbing system generally constitutes an articulated network of vertical or subvertical fractures filled with magma. The occurrence of an outcropping dyke swarm allows us to interpret the geometry of a past Etnean subvolcanic feeding system. The presence of magma chambers, active and fossil, at Mount Etna has been widely documented by geophysical studies (Hirn et al. 1991; Villaseñor et al. 1998; Laigle et al. 2000; Lombardo et al. 2000; Aloisi et al. 2002). In order to explain the abundance of basic-intermediate rocks, petrologists envisaged the occurrence of a large subcrustal magma chamber (cf. Tanguy et al. 1997), together with small intracrustal reservoirs where further differentiation might take place (Armienti et al. 1989, 1994; Trigila et al. 1990; Corsaro et al. 1996; Viccaro et al. 2006; Ferlito et al. 2008a, b). At MC, the existence of subparallel planar intrusions having dips of $55\text{--}75^\circ$ and intrusion intensity of 40% indicate their shallow origin, and therefore their association with small intracrustal reservoirs. In order to understand the geometry of volcanic plumbing systems, Gudmundsson (2006) provided a wide review with numerical simulations of the stresses that control magma chamber ruptures and dyke injections in composite volcanoes and rift zones. In particular, he analyzed systems with single or double magma chamber (at mantle–crust boundary depth and above 4 km), modeling the orientation of the injecting dykes in a homogeneous or anisotropic host rock. The characteristics of the dyke swarm of MC, according to the classification and modeling of Gudmundsson (2006), indicate that this subvolcanic structure could have been fed by a deeper magma chamber (that the present-day Mt. Etna one, located at the mantle–crust boundary; Murru et al. 1999; Aloisi et al. 2002; Chiarabba et al. 2004; Patanè et al. 2006) and connected with a shallower one with a sill-like shape, probably emplaced in a layered crustal segment within the pre-Etnean basement (model represented in Fig. 31 of Gudmundsson 2006). This numerical model fits well with the average dip angle of AD, the intensity of intrusion and the occurrence of normal faults coherent with the dykes; within this frame also the slight variation of $\sim 10^\circ$ in the AD strike and dip could be included. Moreover, the high dip ($55\text{--}75^\circ$) of the dykes would indicate that MC represent an area near the central part of the dykes swarm because in more distal areas, dykes dip more gently (cf. Gautneb et al. 1989; Gudmundsson 2006).

The dyke swarm of MC can be associated to a plumbing system strictly controlled by the regional and/or local tectonic field. This is in agreement with the presence of high angle faults with the same orientation as the dykes. In particular, both faults and AD are E–W oriented, suggesting that the area was subjected to a constant stress field (local and/or regional), with a N–S direction of maximum extension (or minimum compression). Present-day eruptions at Mount Etna occur

preferentially along lateral fractures (oriented NNW–SSE on the southern flank and NE–SW on the northern flank; Lo Giudice et al. 1982; McGuire and Pullen 1989; Monaco et al. 1997, 2005). Their feeding dykes must therefore be aligned along subparallel directions, similar to what was observed in the dykes swarm of MC, which could be considered as an analogue of the present-day shallow plumbing system of Mount Etna.

The N–S direction of maximum extension evidenced in the MC Unit dykes and faults is orthogonal to the E–W one displayed by the present-day Etna volcano (cf. Monaco et al. 1997). This means that during the ancient alkaline phase (220–80 ka), the stress field acting on the area was substantially different. However, this difference need not necessarily have been at a regional scale. In fact, Catalano et al. (2004) hypothesized that NNW–SSE strike-slip tectonics were active during the earlier emissions of sub-alkaline lavas (320–200 ka) and part of the ancient alkaline products (180–100 ka), which produced scattered eruptive centers, developed in locally transtensive zones that were distributed throughout the whole Etnean region. The dyke swarm of MC can therefore be put in the context of tectonics affecting pull-apart structures with E–W fracturing direction.

Considering MC as a shallow portion of a volcano feeding system, we must consider mechanisms that brought it to the surface where it is exposed, in the absence of compressional structures. With this regard, a major change of regional tectonics occurred at 125 ka and was related to the propagation of a normal-fault belt along the Ionian coast of the Catania region and the eastern sectors of the Etnean edifice (Catalano et al. 2004). This caused elevated rates of uplift and associated erosion (cf. Calvari et al. 1998), especially on the eastern flank of present-day Mount Etna, where MC is located. The very fact that MC sticks out in positive topographic relief, in an area dominated by intense erosion, is the ultimate result of the high intensity of intrusion of the dyke swarm: the many more erosion-resistant dykes at MC have in fact prevented the host rock from being totally eroded.

Main characteristics of the Mount Calanna dyke swarm

In order to have a comprehensive picture of the dyke swarm of MC, we should outline some of its most distinctive features. First, the original lithology of the host rock was intensely modified by the intrusion of more than 200 dykes, blurring its characteristics and making difficult for a clear reconnaissance classification. Petrographic observations on some samples of host rock, however, indicate the presence of a mineral assemblage of plagioclase, clinopyroxene, olivine, and opaque oxides with a porphyritic texture, so confirming their volcanic nature. The occurrence of alteration, both at micro- and macroscopic scales, allowed us to distinguish the AD, which constitute the framework of

the dyke swarm of MC, from the UD, which can be related to a later intrusion episode. Although no visible alteration was observed in rocks of the UD, their whole-rock analysis of major elements showed high values of LOI (up to 2.62 wt.%) and of $\text{Fe}_2\text{O}_3/\text{FeO}$ ratio, always >1 . A possible inference that could be made is that a weathering process altered the chemical composition of the UD, a phenomenon quite different from those which affected AD and HR. Indeed, another process of alteration responsible for the present-day features of AD and HR could be related to the occurrence of volcanic fluids circulating during and after the emplacement of the subvolcanic bodies (i.e., hydrothermal processes). This is consistent with the large number of dykes, which continued, after their emplacement, to release gas capable of altering the surrounding rocks (host rock and dykes already intruded).

The density values have been directly measured for the MC rocks. The AD display a broad range of values, from 2,050 to 2,800 kg/m^3 (average, 2,460 kg/m^3). The values of density lower than their fresh dense rock equivalent (2,800 kg/m^3) can be attributed to the presence of vesicles in the dykes, which testifies that they were emplaced above the gas saturation pressure or that there was a post-emplacement crystallization-induced degassing (i.e., second boiling; Boudreau and Simon 2007). The host rocks display homogeneous values with an average density of 2,360 kg/m^3 . Combining these values with the intensity of intrusion of the dyke swarm, we obtain 2,420 kg/m^3 for the entire subvolcanic complex of MC. This value is very close to that proposed for the common Etnean basaltic lavas and pyroclastic rocks (2,400 kg/m^3) by Corsaro and Pompilio (2004a). If the values of density of MC dykes swarm could be extended to represent a similar subvolcanic complex, it would indicate that their occurrence could be underestimated using geophysical studies, in which density is a key parameter. Indeed, recent high-quality seismic tomographies and gravimetric studies show a homogeneous layering of the uppermost portion of the Etnean volcanic succession (<1 – 2 km of depth; e.g., Rollin et al. 2000; Aloisi et al. 2002), which does not reveal any subvolcanic structure. We suggest that in the case of the effective presence of a subvolcanic structure in the roots of the present volcanic edifice, the coincidence of their density values does not allow their differentiation from the volcanic host rock. The occurrence of widespread and shallowly intruded subvolcanic bodies should be investigated through much different geophysical studies, which should take into account not only the densities of the bodies but also other parameters that could reveal fracturing and alteration of the investigated subvolcanic complex (e.g., detailed surface seismic profiles, electric logs, and magnetic susceptibility).

With regard of the depth at which the dyke swarm of MC was originally emplaced, the presence of vesicles, which

especially in some AD reach up to 5 mm in size, indicates that cooling must have occurred at depths shallower than the volatile saturation level of the magma. Assuming dissolved volatile content in the magmas that fed the dykes swarm of MC was similar to those of present-day magmas, and considering that the compositions of AD are generally hawaiitic, the depth of exsolution of about 4 km b.s.l. found by Armienti et al. (1997), Corsaro and Pompilio (2004b), and De Gori et al. (2005) for present-day hawaiitic magmas could also represent the maximum depth of the dyke swarm. Branca et al. (2008) dated the beginning of alkaline magmatism at 220 ka and the ages of rocks of MC as 128.7 ± 3.8 ka and lavas lying above the already eroded surface of the MC at 93.0 ± 3.0 ka. As a consequence, in the time span of less than 40 ka, the dyke swarm should have been uplifted. However, the rates of long-term uplift for the eastern sector of Mount Etna in the last 500 ka were estimated at $0.36\text{--}0.61$ mm year⁻¹ by Di Stefano and Branca (2002) and $0.70\text{--}1.34$ mm year⁻¹ by Antonioli et al. (2006). This implies a moderate uplift of the Val Calanna area (12–50 m) in 40 ka and, even considering high erosion rates, we must conclude that the visible portion of the MC dykes swarm was emplaced at a shallow depth (within 1 km).

Conclusions

A new multidisciplinary study has been carried out on the hill of MC. This isolated outcrop, only 0.7 km² at the outlet of the Valle del Bove, is of great interest to the scientific community because it represents the exposed roots of Mount Etna volcano. In this study, it has been shown that the hill consists primarily of 200 E–W iso-oriented dykes intruded into a volcanic pile. Both dykes and host rock are deeply altered and intruded by more recent and UD. The entire structure is affected by numerous normal faults with orientation parallel to the dykes. These lines of evidence suggest that MC should be considered as a dyke swarm associated to the activity of one or more of the Ancient Alkaline Centers, now eroded and nowhere else exposed. This interpretation has consequences that are important to the understanding of the volcano-tectonic setting and evolution of Mount Etna volcano and justifies the attention given to this small and isolated outcrop: it exposes flaws and weakens the model of gravitational spreading for the eastern flank of Mount Etna volcano that was proposed by Borgia et al. (1992). The characteristics of the dyke swarm and, in particular, the parallelism of the bodies and the high intensity of intrusion suggest that the subvolcanic complex should be considered as an analogue to the uppermost portion of a volcanic plumbing system. The physical constraints on such plumbing systems have been also studied. The extensional stress field was constant during

the emplacement of the dykes and had a N–S direction of maximum extension, orthogonal to the present-day regional and local maximum extension. This was probably a result of transtensional tectonics, which affected the area before 100 ka ago (cf. Catalano et al. 2004). Moreover, measurements of the apparent densities of dykes and host rock have provided values lower than dense rocks with similar compositions. Such values are strikingly similar to those of the outcropping volcanics and the rocks of the Etnean basement, so intrusive bodies might not be recognizable with geophysical studies where density is one of the most important parameters (e.g., seismic tomographies and gravimetry). The detection of a shallow-intruded subvolcanic complex having similar features to the MC dyke swarm could only be recognized through more detailed seismic tomographic and gravimetric studies, but more detailed studies (e.g., detailed shallow seismic profile, magnetic susceptibility, and electric logs) remain to be conducted.

The dyke swarm of MC can be regarded as an exceptional example of a subvolcanic complex exposed on an active and rapidly growing volcano. Further studies on this interesting outcrop can, in our opinion, produce considerable advancements in the understanding of dyke emplacement, not only at Mount Etna but also in other basaltic volcanoes.

Acknowledgements The authors are grateful to Renato Cristofolini for the productive discussions and to Carmelo Monaco for the critical reading of the manuscript. Raffaello Cioni, Carles Soriano, Massimo Pompilio, Agust Gudmundsson, and an anonymous referee are greatly acknowledged for their critical and constructive reviews and suggestions that highly contributed to improve the quality of this manuscript. We are also indebted to Elisabetta Giuffrida and Domenico La Rocca for their precious help in performing major element chemical analyses.

References

- Acocella V, Neri M, Scarlato P (2006) Understanding shallow magma emplacement at volcanoes: orthogonal feeder dikes during the 2002–2003 Stromboli (Italy) eruption. *Geophys Res Lett* 33: L17310
- Aloisi M, Cocina O, Neri G, Orecchio B, Privitera E (2002) Seismic tomography of the crust underneath the Etna volcano, Sicily. *Phys Earth Plan Inter* 134:139–155
- Antonioli F, Kershaw S, Renda P, Rust D, Belluomini G, Cerasoli M, Radtke U, Silenzi S (2006) Elevation of the last interglacial highstand in Sicily (Italy): a benchmark of coastal tectonics. *Quatern Int* 145–146:3–18
- Armienti P, Innocenti F, Petrini R, Pompilio M, Villari L (1989) Petrology and Sr–Nd isotope geochemistry of recent etnean lavas from Mt. Etna: bearing on the volcano feeding system. *J Volcanol Geotherm Res* 39:315–327
- Armienti P, Pareschi MT, Innocenti F, Pompilio M (1994) Effect of magma storage and ascent on the kinetic of crystal growth. The case of the 1991–92 Mt. Etna eruption. *Contrib Miner Petrol* 115:402–414

- Armienti P, Pareschi MT, Pompilio M (1997) Lava textures and time scales of magma storage at Mt. Etna (Italy). *Acta Vulcanol* 9:1–5
- Ben Avraham Z, Grasso M (1990) Collisional zone segmentation in Sicily. *Ann Tecton* 4:131–139
- Borgia A, Ferrari L, Pasquarè G (1992) Importance of gravitational spreading in the tectonic and volcanic evolution of Mount Etna. *Nature* 357:231–235
- Boudreau A, Simon A (2007) Crystallization and degassing in the Basement Sill, McMurdo Dry Valleys, Antarctica. *J Petrol* 48:1369–1386
- Branca S, Coltelli M, Groppelli G (2004) Geological evolution of Etna volcano. In: Bonaccorso A, Calvari S, Coltelli M, Del Negro C, Falsaperla S (eds) *Mt. Etna: volcano laboratory*, vol 143. AGU Geophysical Monograph Series, Washington, pp 49–63
- Branca S, Coltelli M, De Beni E, Wijbrans J (2008) Geological evolution of Mount Etna volcano (Italy) from earliest products until the first central volcanism (between 500 and 100 ka ago) inferred from geochronological and stratigraphic data. *Int J Earth Sci* 97:135–152
- Calvari S, Groppelli G, Pasquarè G (1994) Preliminary geological data on the south-western wall of the Valle del Bove, Mt. Etna, Sicily. *Acta Vulcanol* 5:15–30
- Calvari S, Tanner LH, Groppelli G (1998) Debris-avalanche deposits of the Milo Lahar sequence and the opening of the Valle del Bove on Etna volcano (Italy). *J Volc Geotherm Res* 87:193–209
- Catalano S, Torrisi S, Ferlito C (2004) The relationship between Late Quaternary deformation and volcanism of Mt. Etna (eastern Sicily): new evidences from the sedimentary substratum in the Catania region. *J Volcanol Geotherm Res* 132:311–314
- Chiarabba C, De Gori P, Patanè D (2004) The Mt. Etna plumbing system: the contribution of seismic tomography. In: Bonaccorso A, Calvari S, Coltelli M, Del Negro C, Falsaperla S (eds) *Mt. Etna: volcano laboratory*, vol 143. AGU Geophysical Monograph Series, Washington, pp 191–204
- Coltelli M, Garduño VH, Neri M, Pasquarè G, Pompilio M (1994) Geology of the northern wall of the Valle del Bove, Mt. Etna (Sicily). *Acta Vulcanol* 5:55–68
- Coltelli M, Del Carlo P, Vezzoli L (2000) Stratigraphic constraints for explosive activity in the past 100 ka at Etna volcano, Italy. *Int J Earth Sci* 89:665–677
- Corazzato C, Francalanci L, Menna M, Petrone CM, Renzulli A, Tibaldi A, Vezzoli L (2008) What controls sheet intrusion in volcanoes? Structure and petrology of the Stromboli sheet complex, Italy. *J Volcanol Geotherm Res* 173:25–54
- Corsaro RA, Cristofolini R (1996) Geology, geochemistry and mineral chemistry of tholeiitic to transitional Etnean magmas. *Acta Vulcanol* 9:55–66
- Corsaro RA, Pompilio M (2004a) Buoyancy-controlled eruption of magmas at Mt. Etna. *Terra Nova* 16:16–22
- Corsaro RA, Pompilio M (2004b) Magma dynamics in the shallow plumbing system of Mt. Etna as recorded by compositional variations in volcanics of recent summit activity (1995–1999). *J Volcanol Geotherm Res* 137:55–71
- Corsaro RA, Cristofolini R, Patanè G (1996) The 1669 eruption at Mount Etna: chronology, petrology and geochemistry, with inferences on the magma source and ascent mechanisms. *Bull Volc* 58:348–358
- Cristofolini R, Lentini F, Patanè G, Rasà R (1979) Integrazione di dati geologici, geofisici e petrologici per la stesura di un profilo crostale in corrispondenza dell'Etna. *Boll Soc Geol Ital* 98:239–247
- Cristofolini R, Corsaro RA, Ferlito C (1991) Variazioni petrochimiche nella successione etnea: un riesame in base ai dati da campioni di superficie e da sondaggi. *Acta Vulcanol* 1:25–37
- De Beni E, Wijbrans JR, Branca S, Coltelli M, Groppelli G (2005) New results of Ar-40/Ar-39 dating constrain the timing of transition from fissure-type to central volcanism at Mount Etna (Italy). *Terra Nova* 17:292–298
- De Gori P, Chiarabba C, Patanè D (2005) Qp structure of Mount Etna: constraints for the physics of the plumbing system. *J Geophys Res Solid Earth* 110:B05303
- Di Stefano A, Branca S (2002) Long-term uplift rate of the Etna volcano basement (southern Italy) based on biochronological data from Pleistocene sediments. *Terra Nova* 14:61–68
- D'Orazio M, Tonarini S, Innocenti F, Pompilio M (1997) Northern Valle del Bove volcanic succession (Mt. Etna, Sicily): petrography, geochemistry and Sr-Nd isotope data. *Acta Vulcanol* 9:73–86
- Ferlito C, Cristofolini R (1989) Geologia dell'area sommitale dell'Etna. *Boll Acc Gioenia Sci Nat Catania* 22:357–380
- Ferlito C, Cristofolini R (1991) Evidenze di corpi subvulcanici poco profondi nella successione etnea lungo le pareti occidentali della Valle del Bove. *Mem Soc Geol Ital* 47:485–493
- Ferlito C, Viccaro M, Cristofolini R (2008a) Volatile-induced magma differentiation in the plumbing system of Mt. Etna volcano (Italy): evidence from glass in tephra of the 2001 eruption. *Bull Volc* 70:455–473
- Ferlito C, Coltorti M, Cristofolini R, Giacomoni PP (2008b) The contemporaneous emission of low-K and high-K trachybasalts and the role of the NE Rift during the 2002 eruptive event, Mt. Etna, Italy. *Bull Volcanol*. doi:10.1007/s00445-008-0243-9
- Ferrari L, Calvari S, Coltelli M, Innocenti F, Pasquarè G, Pompilio M, Vezzoli L, Villa I (1989) Nuovi dati geologici e strutturali sulla Valle di Calanna, Etna: implicazioni per l'evoluzione del vulcanismo etneo. *Boll GNV* 2:849–860
- Finetti I (1982) Structure, stratigraphy and evolution of the Mediterranean Sea. *Boll Geof Teor Appl* 15:263–341
- Franzini M, Leoni L, Saitta M (1972) A simple method to evaluate the matrix effect in X-ray fluorescence analysis. *X-ray Spectrum* 1:151–154
- Gautneb H, Gudmundsson A (1992) Effect of local and regional stress field on sheet emplacement in West Iceland. *J Volcanol Geotherm Res* 51:339–356
- Gautneb H, Gudmundsson A, Niels O (1989) Structure, petrochemistry and evolution of a sheet swarm in an Icelandic central volcano. *Geol Mag* 126:659–673
- Gillot PY, Kieffer G, Romano R (1994) The evolution of Mount Etna in the light of potassium-argon dating. *Acta Vulcanol* 5:81–87
- Gudmundsson A (2006) How local stress control magma-chamber ruptures, dyke injections, and eruptions in composite volcanoes. *Earth Sci Rev* 79:1–31
- Hirn A, Nercessian A, Sapin M, Ferrucci F, Wittlinger G (1991) Seismic tomography of Mt. Etna: structure and activity. *Geophys Int* 105:139–153
- Hirn A, Nicolich R, Gallart J, Laigle M, ETNASEIS Scientific Group (1997) Roots of Etna volcano in faults of great earthquakes. *Earth Plan Sci Lett* 148:171–191
- Holcombe Coughlin and Associates (2008) Georient© v.9.4.0. Holcombe Coughlin and Associates, Australia. Available via: <http://www.holcombe.net.au>
- Iuliano T, Mauriello P, Patella D (2002) Looking inside Mount Vesuvius by potential fields integrated probability tomographies. *J Volcanol Geotherm Res* 113:363–378
- Jolly RJH, Sanderson DJ (1995) Variation in the form and distribution of dykes in the Mull swarm, Scotland. *J Struct Geol* 17:1543–1557
- Klausen MB (2004) Geometry and mode of emplacement of the Thverantindur cone sheet swarm, SE Iceland. *J Volcanol Geotherm Res* 138:185–204
- Klausen MB (2006) Geometry and mode of emplacement of dike swarms around the Birnudalstindur igneous centre, SE Iceland. *J Volcanol Geotherm Res* 151:340–356
- Klerckx J (1970) La caldera de la Valle del Bove: sa signification dans l'évolution de l'Etna (Sicile). *Bull Volcanol* 247:726–737

- Laigle M, Hirn A, Sapin M, Lépine J, Diaz J, Gallart J, Nicolich R (2000) Mount Etna dense array local earthquake P and S tomography and implications for volcanic plumbing. *J Geophys Res* 105:21,633–21,646
- Lanzafame G, Vestch P (1985) Les dykes de la Valle del Bove (Etna, Sicile) et le champ de constraints régionales. *Rev Geol Dinam Geogr Phys* 26:147–156
- Le Maitre RW (2002) A classification of igneous rocks and glossary of terms. Cambridge University Press, Cambridge
- Lentini F (1982) The geology of the Mt. Etna basement. *Mem Soc Geol Ital* 23:7–25
- Lo Giudice E, Patanè G, Rasà R, Romano R (1982) The structural framework of Mount Etna. *Mem Soc Geol Ital* 23:125–158
- Lombardo G, Barbano MS, Costanzo S (2000) Anomalies of seismic wave propagation at Mt. Etna Volcano, Italy. *J Volcanol Geotherm Res* 101:171–182
- Lopez M, Pompilio M, Rotolo SG (2006) Petrology of some amphibole-bearing volcanics of the pre-Ellittico period (102–80 ka), Mt. Etna. *Period Min* 75:151–170
- Marinoni LB (2001) Crustal extension from exposed sheet intrusions: review and method proposal. *J Volcanol Geotherm Res* 107:27–46
- Marinoni LB, Gudmundsson A (2000) Dykes, faults and palaeostresses in the Teno and Anaga massifs of Tenerife (Canary Islands). *J Volcanol Geotherm Res* 103:83–103
- Mattia M, Aloisi M, Di Grazia G, Gambino S, Palano M, Bruno V (2008) Geophysical investigations of the plumbing system of Stromboli volcano (Aeolian Islands, Italy). *J Volcanol Geotherm Res* 176:529–540
- McGuire WJ (1982) Evolution of the Etna volcano: information from the southern wall of the Valle del Bove caldera. *J Volcanol Geotherm Res* 13:241–271
- McGuire WJ, Pullen AD (1989) Location and orientation of eruptive fissures and feeder-dykes at Mount Etna: influence of gravitational and regional tectonic stress regimes. *J Volcanol Geotherm Res* 38:325–344
- Merle O, Borgia A (1996) Scaled experiments of volcanic spreading. *J Geophys Res-Sol Earth* 101:13805–13817
- Monaco C, Tapponier P, Tortorici L, Gillot PY (1997) Late Quaternary slip rates on the Acireale-Piedimonte normal faults and tectonic origin of Mt. Etna (Sicily). *Earth Planet Sci Lett* 147:125–139
- Monaco C, Catalano S, Cocina O, De Guidi G, Ferlito C, Gresta S, Musumeci C, Tortorici L (2005) Tectonic control on the eruptive dynamics at Mt. Etna volcano (Sicily) during the 2001 and 2002–2003 eruptions. *J Volcanol Geotherm Res* 144:211–233
- Monaco C, De Guidi G, Catalano S, Ferlito C, Tortorici G, Tortorici L (2008) Morphotectonic map of Mt. Etna (1:75,000). INGV-DPC 2005–2007 Project
- Morimoto N, Fabries J, Ferguson AK, Ginzburg IV, Ross M, Seifert FA, Zussmann J, Aoki K, Gottardi G (1998) Nomenclature of pyroxenes. *Am Mineral* 73:1123–1133
- Murru M, Console R, Falcone G, Montuori C, Sgroi T (1999) Spatial mapping of the b value at Mount Etna, Italy, using earthquake data recorded from 1999 to 2005. *J Geophys Res Solid Earth* 112:B12303
- Nazzareni S, Busà T, Cristofolini R (2003) Magmatic crystallisation of Cr-Al diopside and Al-Fe³⁺ diopside from the ancient alkaline basalts (Mt. Etna, Sicily). *Eur J Mineral* 15:81–93
- Patanè D, Barberi G, Cocina O, De Gori P, Chiarabba C (2006) Time-resolved seismic tomography detects magma intrusions at Mount Etna. *Science* 313:821–823
- Porreca M, Acocella V, Massimi E, Mattei M, Funicello R, De Benedetti AA (2006) Geometric and kinematic features of the dike complex at Mt. Somma, Vesuvio (Italy). *Earth Planet Sci Lett* 245:389–407
- Rollin PJ, Cassidy J, Locke CA, Rymer H (2000) Evolution of the magmatic plumbing system at Mt. Etna: new evidence from gravity and magnetic data. *Terra Nova* 12:193–198
- Romano R (1982) Succession of the volcanic activity in the Etnean area. *Mem Soc Geol Ital* 23:27–48
- Romano R, Guest JE (1979) Volcanic geology of the summit and northern flank of Mount Etna, Sicily. *Boll Soc Geol It* 98:189–215
- Romano R, Sturiale C (1975) Geologia della tavoletta “Monte Etna Sud” (F. 262 – III SO). *Boll Soc Geol Ital* 94:1109–1148
- Tanguy JC, Condomines M, Kieffer G (1997) Evolution of the Mount Etna magma: constraints on the present feeding system and eruptive mechanism. *J Volcanol Geotherm Res* 75:221–250
- Trigila R, Spera FJ, Aurisicchio C (1990) The 1983 Mount Etna eruption: thermochemical and dynamical inferences. *Contrib Miner Petrol* 104:594–608
- Viccaro M, Ferlito C, Cortesogno L, Cristofolini R, Gaggero L (2006) Magma mixing during the 2001 event at Mount Etna (Italy): effects on the eruptive dynamics. *J Volcanol Geotherm Res* 149:139–159
- Villaseñor A, Benz HM, Filippi L, De Luca G, Scarpa R, Patanè G (1998) Three-dimensional P-wave velocity structure of Mt. Etna, Italy. *Geophys Res Lett* 25:1975–1978
- Walker GPL (1992) “Coherent intrusion complexes” in large basaltic volcanoes—a new structural model. *J Volcanol Geotherm Res* 50:41–54
- Wezel FC (1967) I terreni quaternari del substrato dell'Etna. *Atti Accad Gioenia Sci Nat Catania* 6:271–282